On Asteroseismic Probes of Convective Core Boundary Mixing in RR Lyrae Stars

MARIA KOROLIK [ID],[1] EARL P. BELLINGER [ID],[1] EBRAHEEM FARAG [ID],[1] SELIM KALICI [ID],[1] AND CHRISTOPHER LINDSAY [ID][1]

[1]*Department of Astronomy, Yale University, CT, USA*

ABSTRACT

Convective boundary mixing in stellar interiors remains an outstanding problem in stellar astrophysics. Here we examine how different convective boundary mixing schemes affect the evolution and gravity-mode pulsations of core helium-burning RR Lyrae variable stars. We use the stellar evolution software instrument MESA and the stellar oscillation code GYRE to investigate the differences in gravity-mode signatures arising from variations in convective boundary mixing schemes. We find that distinct convective boundary mixing treatments yield measurable differences in gravity-mode period spacings, with models incorporating overshoot clearly distinguishable from those without. However, variations in the strength of overshoot produce less discernible effects. We find the differences in gravity mode period spacing due to different convective boundary mixing treatments are larger than those arising from variations in mass and metallicity. Distinct convective boundary mixing treatments also yield measurable differences in the rate of change of the fundamental period. We also find that RR Lyrae stars produced through envelope stripping from a binary star companion have distinct asteroseismic characteristics, thereby offering means to confirm that high-metallicity RR Lyrae evolved through this channel. These results suggest that gravity mode period spacings, potentially measurable with high-precision photometric missions, can constrain convective boundary mixing processes in RR Lyrae stars and thus would improve our understanding of their internal structure and evolutionary history.

Keywords: Asteroseismology, RR Lyrae variable stars, Stellar evolution

1. INTRODUCTION

Understanding stellar convection remains a critical challenge in stellar astrophysics. Precise modeling, particularly near convective boundaries, is essential for accurately predicting stellar lifetimes, chemical enrichment, and observable stellar pulsations (Sweigart & Demarque 1973; Castellani et al. 1985; Kippenhahn et al. 2013; Constantino et al. 2017).

Previous theoretical studies have emphasized the impact of convective boundary mixing (CBM) schemes on stellar evolution predictions, highlighting differences in evolutionary tracks, lifetimes, and internal structure (Gabriel et al. 2014; Constantino et al. 2017; Paxton et al. 2019). Despite these advancements, uncertainties remain concerning the physical validity of convection phenomena such as semiconvection, overshoot, and breathing pulses in core helium-burning stars (Castellani et al. 1985; Ostrowski et al. 2021; Córsico & Althaus 2024). Observational constraints derived from precise asteroseismic measurements offer a pathway to resolving these uncertainties, refining convective modeling and improving stellar evolutionary models.

Gravity modes (g-modes) are particularly useful for probing stellar interiors as they are sensitive to the internal chemical and structural gradients, such as those near convective boundaries (e.g., Miglio et al. 2008; Aerts et al. 2010; Montalbán et al. 2013). Recent advancements in space-based photometry, such as the NASA TESS (Ricker et al. 2015) and *Kepler* (Borucki et al. 2010) missions as well as the forthcoming ESA PLATO (Rauer et al. 2016, 2025) mission, enable precise measurements of gravity mode period spacings (e.g., Charpinet et al. 2011; Reed et al. 2011; Pedersen et al. 2018), greatly enhancing our capability to investigate convective boundary mixing (e.g., Miglio et al. 2008; Townsend & Teitler 2013).

RR Lyrae are old, core helium-burning, Population II variable stars in the classical instability strip that serve as valuable probes for stellar astrophysics due to their well-established pulsation properties (e.g., Jurcsik et al. 2015; Netzel et al. 2023b). Like Cepheid variable stars, they exhibit a period-luminosity relationship

in some wavelengths, allowing them to be used as standard candles (Longmore et al. 1986). These stars pulsate predominantly in radial modes, but recent studies have demonstrated the possible presence of additional low-amplitude non-radial modes, including gravity modes, providing an opportunity to explore their deep internal structures through asteroseismology (Dziembowski 2016; Chadid 2022; Netzel et al. 2023a).

In this study, we investigate how various CBM schemes affect the internal structure, evolution, and gravity mode pulsations of RR Lyrae stars. We utilize the MESA stellar evolution software instrument (Paxton et al. 2011, 2013, 2015, 2018, 2019; Jermyn et al. 2023) and the stellar oscillation code GYRE (Townsend & Teitler 2013; Townsend et al. 2018) to analyze the impact of different CBM schemes on the observable pulsation properties of stellar models (Section 2). Different CBM schemes result in variations in both the stellar structure and evolution (Section 3), as well as in the radial pulsations of RR Lyrae stars (Section 4). Our findings demonstrate that different CBM schemes result in clear signatures in the gravity mode period spacings of stellar models (Section 5) and that the differences in these signatures are insensitive to changes in mass and metallicity (Section 6). Finally, we show that gravity mode period spacings can also be used to distinguish between single and binary evolution RR Lyrae (Section 7).

1.1. *Convection*

Core helium-burning stars such as RR Lyrae produce carbon through the triple-α reaction and oxygen through the $^{12}\mathrm{C}(\alpha,\gamma)^{16}\mathrm{O}$ reaction in their convective cores. This creates a sharp discontinuity in the chemical abundance gradient at the edge of the convective region. The edge of the convective boundary is sensitive to changes in the abundance gradient due to its dependence on the opacity (Castellani et al. 1971, 1985), therefore, the position of the convective core boundary is highly unstable to any perturbation. Because the boundary is typically defined as the point of zero acceleration, there is strong physical reasoning for convective overshoot to extend the convective region (Herwig et al. 1999; Deng & Xiong 2008). Additional mixing past the extent of the convective boundary due to overshoot mixes in fresh material and changes the chemical abundance and thermodynamic profile. This in turn changes the position of the convective boundary (e.g., Constantino et al. 2017).

There are two different criteria used to determine whether or not a region of a star is unstable to convection. The Ledoux (1947) criterion for stability is defined as:

$$\nabla_{\mathrm{rad}} < \nabla_{\mathrm{ad}} + \frac{\phi}{\delta}\nabla_{\mu}, \tag{1}$$

with

$$\nabla = \frac{\mathrm{d}\ln T}{\mathrm{d}\ln P}, \quad \phi = \frac{\partial \ln \rho}{\partial \ln \mu}, \quad \delta = \frac{\partial \ln \rho}{\partial \ln T}. \tag{2}$$

In a region with homogenous chemical composition, this reduces to the Schwarzschild (1906) criterion:

$$\nabla_{\mathrm{rad}} < \nabla_{\mathrm{ad}}. \tag{3}$$

In the presence of a discontinuity in the mean molecular weight, a small region of the star just above the discontinuity becomes convectively unstable (Ledoux 1947). This region of semiconvection and its efficiency in mixing can vary the lifetime of a core helium-burning star by bringing in extra helium to the helium-burning region (Castellani et al. 1985).

Models of core helium-burning stars with convective overshoot also exhibit behavior called "breathing pulses" as their convective core experiences episodes of sudden growth (Castellani et al. 1985). As the mass of the convective core increases due to overshoot, the helium composition of the core is enriched; even a small amount of enrichment causes a large increase in the energy generation due to the triple-α reaction's sensitivity to temperature and chemical composition (Sweigart & Demarque 1973). The increase in helium burning subsequently increases the opacity in the core, raising ∇_{rad}, thereby increasing the extent of convective overshoot necessary to match ∇_{rad} and ∇_{ad} at the convective boundary. This instability leads to sudden growth of the convective core.

These breathing pulses can significantly prolong the helium-burning lifetime of a star by continuously increasing the supply of helium available for burning. However, it is unclear if these breathing pulses are physical phenomena or if they are merely a numerical artifact (Castellani et al. 1985). The time spent in the core helium-burning phase has important implications for topics in stellar astrophysics, including the lifespan of stars, and a wider range of fields, such as galaxy evolution, star formation, and more (Huber et al. 2019). Therefore, developing empirically-tested constraints on the convective boundaries of core helium-burning stars such as RR Lyrae is critical to providing context for many fields of astrophysics.

Asteroseismology offers a potential avenue to probe this convective boundary mixing and resolve this conundrum. Previous studies of different types of oscillators, such as slowly pulsating B stars, have discussed the power of gravity modes to quantify the accuracy of

different CBM schemes (e.g., Miglio et al. 2008; Pedersen et al. 2018).

In addition to asteroseismology, a common probe of the extent of convective boundaries within stars is measuring the observed ratio of the number of stars on the asymptotic giant branch to the number of stars on the horizontal branch (Bressan et al. 1986). Convective overshooting extends the core helium-burning lifetime, thus increasing the number of stars on the horizontal branch relative to the number of post-horizontal branch stars (e.g., Bertelli et al. 1984; Constantino et al. 2016).

1.2. Variable Stars

Stars typically pulsate in a combination of two types of oscillation modes: pressure modes and gravity modes. These modes differ in their restoring force: pressure-mode oscillations are restored by the star's pressure gradient, whereas gravity-mode oscillations are restored by the buoyancy force.

Gravity modes are confined to radiative regions of the star. They are restored by buoyancy, which is inherently three-dimensional; hence, there are no radial ($\ell = 0$) gravity modes.

Gravity modes generally tend to probe deeper into the star than pressure modes, making them a critical tool for understanding the physics of the deep stellar interior.

Gravity modes of the same degree and high radial order are nearly equally spaced in period (Tassoul 1980). The asymptotic period spacing of a given degree ℓ can be calculated as follows:

$$\Delta\Pi_\ell = \frac{2\pi^2}{\sqrt{\ell(\ell+1)}} \left(\int \frac{N}{r} dr \right)^{-1}, \qquad (4)$$

where the Brünt-Väisälä (buoyancy) frequency N is defined as

$$N^2 = g \left(\frac{1}{\Gamma_1} \frac{d\ln P}{dr} - \frac{d\ln\rho}{dr} \right), \qquad (5)$$

where g is gravity, ℓ is the mode order, and Γ_1 is the first adiabatic exponent, $\Gamma_1 = \left(\frac{\partial \ln P}{\partial \ln \rho} \right)_{\rm ad}$.

The asymptotic period spacing is often observed for red giant stars, which typically exhibit a wide range of mixed modes. This mixed mode period spacing can be used to distinguish core helium-burning stars from shell hydrogen-burning stars (Bedding et al. 2011). Comparing the theoretically derived asymptotic period spacing with the observed one allows us to place constraints on the internal structure of the star. The asymptotic period spacing depends on the mass of the convective core; thus, it is highly sensitive to the strength of type of overshoot employed. Discrepancies between observed and predicted asymptotic period spacings allow better constraints on convective boundary modeling (Constantino et al. 2015).

1.3. RR Lyrae Variable Stars

RR Lyrae variable stars have a typical fundamental period of less than a day; some RR Lyrae stars also exhibit phase and amplitude modulation of their fundamental period due to the Blazhko effect (Blažko 1907). Most RR Lyrae pulsate in the fundamental mode (RRab stars) or in the first overtone (RRc stars), or both at the same time (RRd stars) (Netzel et al. 2023b). Many RR Lyrae stars have been observed to pulsate with low-amplitude, short-period signals at a period ratio ~ 0.61 to the first overtone (e.g., Montalbán et al. 2013; Jurcsik et al. 2015; Smolec et al. 2017b). A possible explanation for this signal is harmonics of non-radial modes with $\ell = 8$, $\ell = 9$ (Dziembowski 2016).

While the pulsations of RR Lyrae stars are dominated by the fundamental mode and (sometimes) their first overtone (pressure modes with $\ell = 0$, $n = 1, 2$), RR Lyrae stars can also potentially pulsate in many non-radial ($\ell > 0$) modes, including gravity modes. Gravity modes were reported to be detected in the RR Lyrae star HH Puppis (Chadid 2022), a A3II/III (Stock & Wroblewski 1972) star with $T_{\rm eff} \sim 6400$ K and [Fe/H] ~ -1.50 (Gilligan et al. 2021). Chadid (2022) found the fundamental period to be 9.38 hours.

While RR Lyrae can likely pulsate in gravity modes, they are difficult to detect for several reasons. First, the amplitudes of the radial pulsations in RR Lyrae are orders of magnitude larger than the amplitudes of gravity modes. Second, removing the signals of the radial pulsations is challenging due to many RR Lyrae stars exhibiting the Blazhko effect, which causes period and amplitude modulations. Finally, the large amplitude radial modes may couple with other modes, not only resonantly driving and damping them but also making the outer boundary condition time-dependent, potentially changing the characteristics of the non-radial modes.

2. MESA AND GYRE MODELS

2.1. Stellar evolution

In this work, we used the one-dimensional stellar evolution software instrument MODULES FOR EXPERIMENTS IN STELLAR ASTROPHYSICS (MESA version r24.03.1, Paxton et al. 2011, 2013, 2015, 2018, 2019; Jermyn et al. 2023). The MESA equation of state is a blend of the OPAL (Rogers & Nayfonov 2002), FreeEOS (Irwin 2004), and Skye (Jermyn et al. 2021) equations of state. Radiative opacities are primarily from OPAL (Iglesias & Rogers 1993, 1996), with

low-temperature data from Ferguson et al. (2005) and the high-temperature, Compton-scattering dominated regime by Poutanen (2017). Electron conduction opacities are from Cassisi et al. (2007) and Blouin et al. (2020). Nuclear reaction rates are from JINA REACLIB (Cyburt et al. 2010), NACRE (Angulo et al. 1999) and additional tabulated weak reaction rates Fuller et al. (1985); Oda et al. (1994); Langanke & Martínez-Pinedo (2000). Screening is included via the prescription of Chugunov et al. (2007), and thermal neutrino loss rates are from Itoh et al. (1996).

MESA use time-dependent convection, as described in Jermyn et al. (2023), which asymptotically reproduces the Cox & Giuli (1968) description of mixing length theory in the limit of long time scales. Time-dependent convection, derived from Kuhfuss (1986), is a Reynolds-averaged Navier-Stokes (RANS) model of convection that aims to describe the mean flow characteristics of convection. Either the Ledoux criterion or the Schwarzschild criterion for convection can be used in MESA, and both are explored in this work. MESA's implementation of overshoot allows for either step overshoot or exponential overshoot. In this work, step overshoot is used. In step overshoot, the diffusion coefficient from mixing length theory is taken from a distance $f_0 \cdot H_p$ (where H_p is the pressure scale height, $H_p = P\rho/g$) into the convective region from the boundary. The diffusion coefficient from the convective region is then applied to model cells above the convective boundary up to a distance $\alpha_{\mathrm{ov}} \cdot H_p$ above the convective boundary. α_{ov} is a free parameter, also labeled f_{ov} in the MESA documentation (Paxton et al. 2011). In addition to overshoot, we also investigate MESA's premixing scheme (Paxton et al. 2019).

2.2. Stellar oscillations

To calculate the oscillation modes of the star as it evolves, we use the stellar oscillation code GYRE (Townsend & Teitler 2013; Townsend et al. 2018).

We scan for fundamental ($\ell = 0, n = 1$) modes using the non-adiabatic oscillation equations in the frozen convection approximation to find when the fundamental mode is excited to determine the boundaries of the instability strip for our models. This is reliable at the blue edge of the instability strip but unreliable at the red edge of the instability strip (where a convective envelope may develop) because this approximation ignores the interaction between pulsations and convection. Furthermore, while it accounts for the Eddington opacity valve (κ-mechanism) exciting radial oscillations, it does not account for the stochastic excitation of gravity modes using turbulent convection.
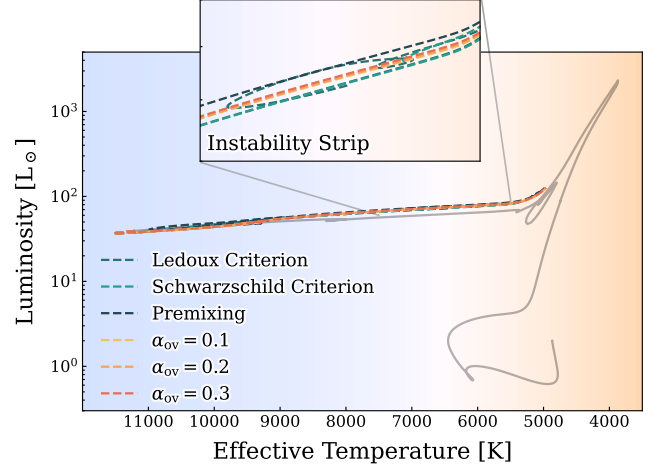

Figure 1. Stellar evolutionary tracks on the Hertzsprung-Russell diagram with the common track (preceding the helium flash) in black and the six tracks with different CBM schemes moving from blue to red across the horizontal branch. An inset diagram (5500 K < T < 7500 K; 60 L$_\odot$ < L < 90 L$_\odot$) shows the stellar evolutionary tracks during the classical instability strip. The background is colored by spectral type. The different CBM schemes show little difference in their evolutionary tracks across the horizontal branch.

2.3. Stellar models

For this study, a model of initial mass M = 0.83 M$_\odot$ with metallicity Z = 0.001, helium abundance Y = 0.25, a Reimers cool RGB wind scheme with a scaling factor of 0.5 (typical parameters for RR Lyrae stars, Fadeyev (2019); Das et al. (2020)), and mixing length $\alpha_{\mathrm{MLT}} = 2$ was evolved until the helium flash (at which point it was 11.69 Gyr, 0.59 M$_\odot$). Subsequent models were started at the helium flash and evolved to core helium depletion using different CBM schemes; see Table 1 for details. The tracks can be seen on the Hertzsprung-Russell diagram in Figure 1.

We also construct of an additional model of initial mass M = 0.88 M$_\odot$ and metallicity Z = 0.002 for comparison, with the other parameters kept the same. It was evolved until the helium flash (at which point it was 10.42 Gyr, 0.63 M$_\odot$). Subsequent models were started at the helium flash and evolved to core helium depletion using different CBM schemes prescriptions; see Table 1 for details. These tracks are further discussed in Section 6.

Our code and models are publicly available[1].

---

[1] https://github.com/mkorolik/RR-Lyrae-Convective-Boundary-Mixing (Korolik 2025)

Table 1. Summary of stellar evolution tracks analyzed in this study. All models use $Y = 0.25$, a Reimers RGB wind with $\eta_R = 0.5$, and mixing–length parameter $\alpha_{\mathrm{MLT}} = 2.0$. "SC" is the Ledoux semiconvection efficiency; "PM" indicates the premixing scheme; overshooting uses a step form with fixed $f_0 = 0.05$ and the listed step length α_{ov}.

Track	$\mathrm{M}_i/\mathrm{M}_\odot$	Z	Criterion	SC	PM	α_{ov}	Notes
1-1	0.83	0.001	Ledoux	0.1	—	—	baseline
1-2	0.83	0.001	Schwarzschild	—	—	—	no semiconvection
1-3	0.83	0.001	Ledoux	0.1	✓	—	premixing scheme
1-4	0.83	0.001	Ledoux	0.1	—	0.10	step overshoot
1-5	0.83	0.001	Ledoux	0.1	—	0.20	step overshoot
1-6	0.83	0.001	Ledoux	0.1	—	0.30	step overshoot
2-1	0.88	0.002	Ledoux	0.1	—	—	baseline
2-2	0.88	0.002	Schwarzschild	—	—	—	no semiconvection
2-3	0.88	0.002	Ledoux	0.1	✓	—	premixing scheme
2-4	0.88	0.002	Ledoux	0.1	—	0.10	step overshoot
2-5	0.88	0.002	Ledoux	0.1	—	0.20	step overshoot
2-6	0.88	0.002	Ledoux	0.1	—	0.30	step overshoot

3. STELLAR STRUCTURE

Different CBM schemes result in different internal structures. The evolution of the internal structures for the models explored in this study are shown in Figure 2. Both models without overshooting or premixing (Tracks 1-1 and 1-2) show minimal change in the convective core size until near core helium depletion. All models with step overshooting display a splitting of the convective region above the core. They appear similar to the breathing pulses described in Section 1 and may potentially arise as numerical artifacts (Castellani et al. 1985; Ostrowski et al. 2021).

While the shape of the evolution of the convective core does not differ between the models without overshoot or premixing, the size (in mass) of the convective core and the age of core helium depletion do differ. The Ledoux criterion model (Track 1-1) has a convective core boundary at 0.119 $\mathrm{M}_\odot$, whereas the Schwarzschild criterion model (Track 1-2) has its convective core boundary at 0.125 $\mathrm{M}_\odot$ (for the same total star mass of 0.59 $\mathrm{M}_\odot$). The models differ in age at core helium exhaustion by ~ 2 Myr. More notably, these two models differ more significantly in age from the models with overshoot or premixing, with a difference of ~ 40-60 Myr. Models without overshoot or premixing (Tracks 1-1 and 1-2), display a convective region that is smaller in extent than the helium-burning core. The convection fails to bring in any new helium to the core; it mixes the existing helium and helium fusion products homogeneously throughout the core. In the models with premixing or overshoot (Tracks 1-3 through 1-6), the convective region extends beyond the helium-burning core. This allows the con-

vection to continuously mix in new helium into the core, increasing the available amount of helium and thus extending the core helium-burning lifetime.

The effect of this additional helium over time can also be seen in the composition diagram of the different models shown in Figure 3. This figure shows the composition profiles of the models at the age when the fundamental period is roughly 24 hours (almost at the end of the helium-burning lifetime, with core helium abundance $Y_c < 0.01$). At this point, the models all have similarly shaped convective regions that are smaller than the extent of the helium-burning zone. However, these convective regions have significantly different histories, as seen in Figure 2. These different histories show a strong impact on the helium composition profile within the model. The two models without overshoot or premixing (Tracks 1-1 and 1-2) have profiles with two sharp discontinuities: one at the core convective boundary, and one at the hydrogen-burning zone (with a small bump at the base of the hydrogen-burning zone before the discontinuity). The models with premixing or overshoot (Tracks 1-3 through 1-6) show both discontinuities and gradual changes in the helium composition profile. The premixing model (Track 1-3) has a sharp discontinuity above the edge of the convective region within the core helium-burning region. This mass coordinate marks the extent of the farthest overshooting, where the convection was able to continuously add an additional supply of helium to the core fusion. After the helium-burning region, the composition shows a smoother gradient of helium, with a small flat step in the middle which does not appear to correlate with any feature in Figure 2.
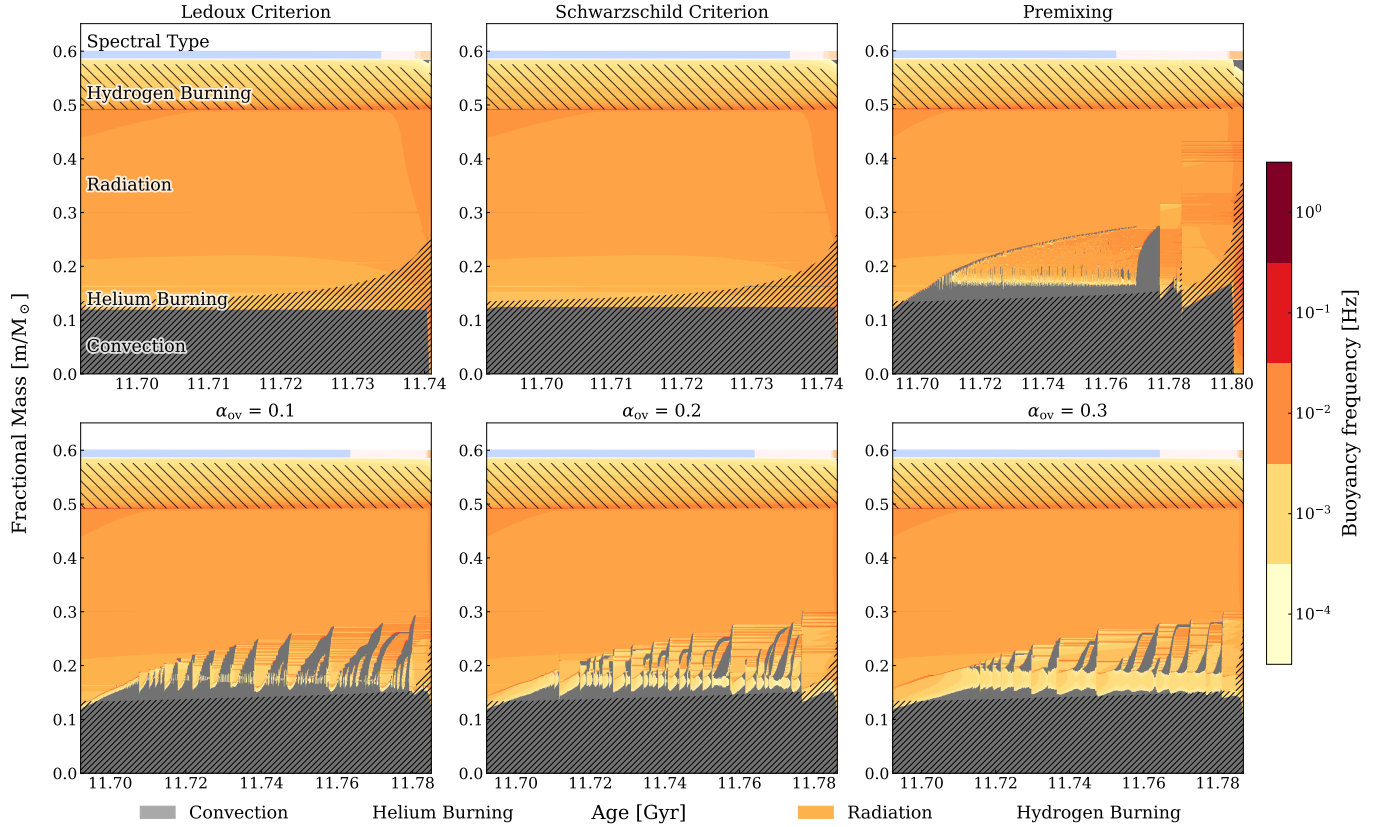
Figure 2. Kippenhahn diagrams of the models, beginning at the onset of core helium burning. The gray regions denote convective regions, and the hatched regions denote the hydrogen-burning shell and the helium-burning core. The color line at the top of each subplot denotes the spectral type of the star. The radiative region is colored by the magnitude of the buoyancy frequency. Helium breathing pulses are seen in the models with step overshoot (bottom row).

Similarly, the models with step overshoot (Tracks 1-4 through 1-6) have a low constant helium composition until the edge of the farthest convection in the star, and then a small discontinuity and a relatively smooth gradient until past the burning zone. Unlike premixing, the models with step overshoot show a longer flat composition profile between the end of convection and the base of the hydrogen-burning region.

When the stellar models reach the classical instability strip, the shapes of the convective regions in the models are very similar, if not identical. However, there is still an observable difference in their pulsations, discussed further in Sections 4 and 5. This difference can be attributed to the different composition profiles resulting from the different histories in convective region profiles. These different composition profiles result in different Brünt-Väisälä frequency profiles as the Brünt-Väisälä frequency is sensitive to changes in molecular weight. Thus, the models will have different gravity mode cavities and different predicted asymptotic period spacings. While the asymptotic period spacing has not been measured yet in RR Lyrae (due to the lack of gravity mode

detections in RR Lyrae), it has been measured precisely with an uncertainty < 1s in red giants and other core helium-burning stars (e.g., Bedding et al. 2011; Mosser et al. 2012a,b), meaning it can be an important tool to detect differences in composition profiles, and thus an important tool to differentiate between different CBM schemes in stellar models.

4. RADIAL OSCILLATIONS

The fundamental period of the star scales inversely with its mean density (Ritter 1880; Eddington 1926). Hence, as the star evolves towards the red edge of the blue loop and its radius expands, the fundamental period increases. Many RR Lyrae stars also pulsate in their first overtone (RRd stars). The ratio of these two periods is often plotted for observed stars in a Petersen diagram. Classical RRd stars form a tight and well-defined progression in the Petersen diagram (Smolec et al. 2017a). Petersen diagrams of observed low-amplitude pulsations can begin to place constraints on the existence of possible observed non-radial pulsations (e.g., Dziembowski 2016; Netzel et al. 2023a).
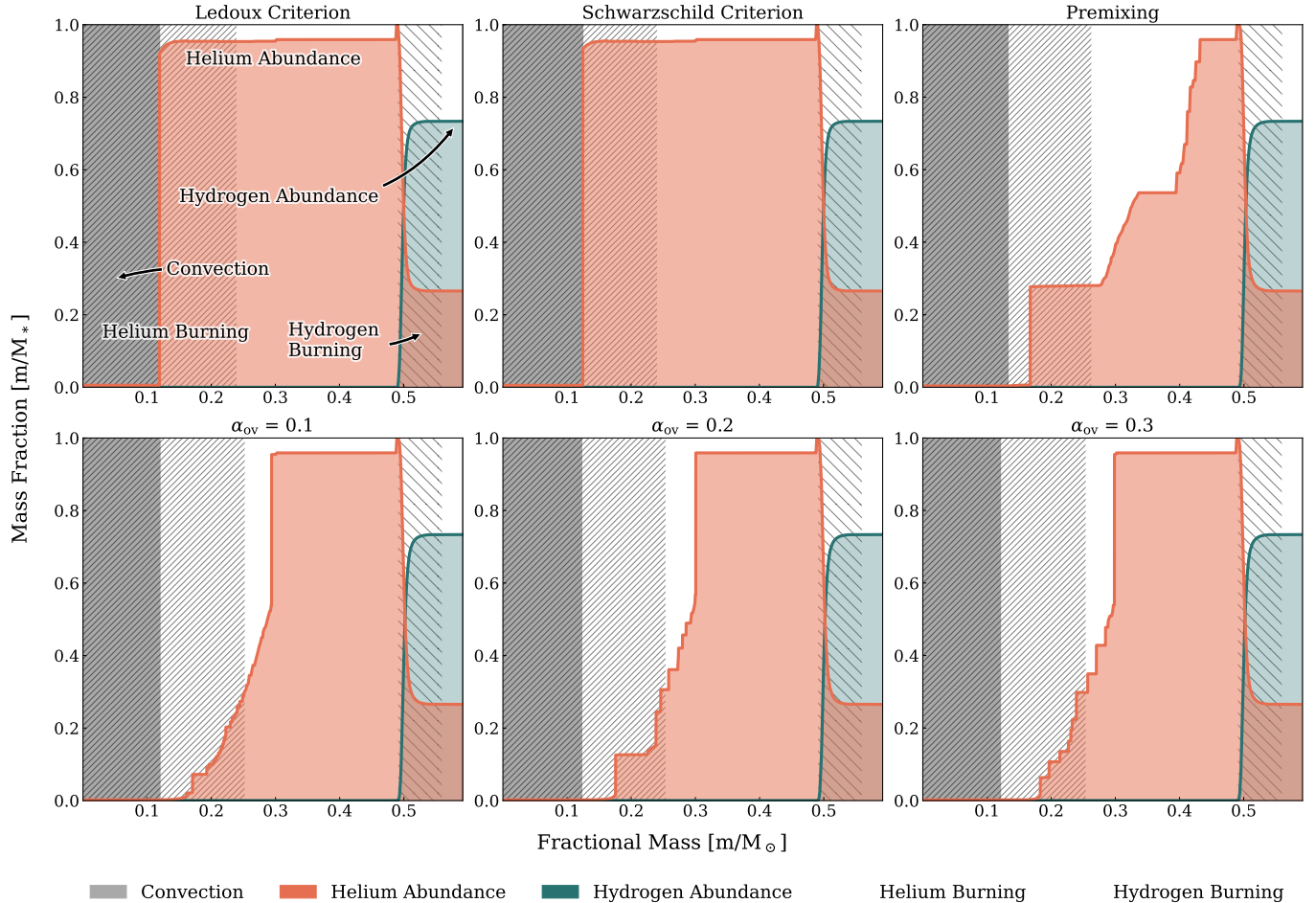
Figure 3. Composition diagram of the models at the age when the fundamental period ~ 24 hours. The orange shaded region shows the helium mass fraction, and the green shaded region shows the hydrogen mass fraction. As in the Kippenhahn diagrams in Figure 2, the gray region denotes convection and the hatched lines denote hydrogen- and helium-burning regions. The models with overshoot show signatures in the helium abundance left over by the convection previously extending farther into the star during the breathing pulses.

The fundamental mode in classical pulsators likely affects all other modes, including the gravity modes discussed later in this work. Due to its large amplitude, other modes may couple to it, as it periodically displaces the outer cavity in which all modes oscillate. This may therefore affect which non-radial modes are excited, and thus which non-radial modes are possible to observe.

The rate of change of the fundamental period also depends on the CBM scheme, as seen in Figure 4. The models without overshoot (Tracks 1-1 and 1-2) have a much slower rate of change throughout their time during core helium burning. The models with overshoot or premixing, however, show a sharp increase in their rate of period change. Measuring the rate of change of the fundamental period of an RR Lyrae star can help not only constrain which CBM scheme can best be used to model it, but also the fraction of time spent during its core helium-burning lifetime. The fundamental period of the star depends on its mean density; thus, for a given point in the Hertzsprung-Russell diagram, stars of the same mass will have the same fundamental period. However, the CBM scheme affects the rate at which a star will move through a given track on the Hertzsprung-Russell diagram. For a given point, while the fundamental period may be the same for models of different CBM schemes, the rate at which that period is changing will differ based on how fast the star moves from the blue edge of the instability strip to the red edge of the instability strip. This is determined by the amount of helium available for burning (i.e., the extent of the core convective zone).

For typical RR Lyrae periods, the difference between the rates of change of the fundamental period is greater than ~ 0.2 d Myr^{-1}, which is observable with long time baselines (e.g., Arellano Ferro et al. 2016, 2018). The fundamental period change rates in these models is a
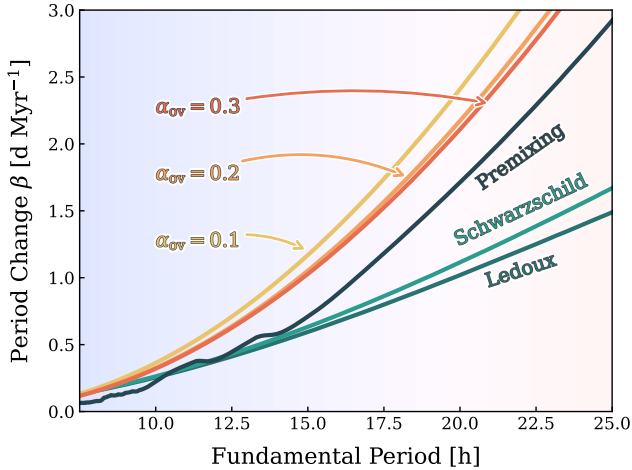
Figure 4. Rate of change of the fundamental period as a function of the fundamental period. For typical RR Lyrae, the fundamental period can be observed to a precision of $\sim 10^{-6}$ days; the difference in fundamental period change here is thus large enough to be detected. The background color shows the spectral type of the star at a given fundamental period.

property of RR Lyrae that may be used to distinguish between different CBM schemes given current observational constraints.

5. GRAVITY MODES

The period spacing between gravity modes of the same angular degree but consecutive radial order depends on the profile of the Brünt-Väisälä frequency. As the Brünt-Väisälä frequency is sensitive to sharp changes in the mean molecular weight, one can expect the period spacing to vary between these different models. The period spacing in both models without overshoot or premixing (Tracks 1-1 and 1-2) are similar to each other as they have nearly identical composition profiles and temperature gradient profiles. However, these two models differ significantly from the four models with premixing or overshoot in their composition profiles, as described above. We investigate this by determining the models' asymptotic period spacing through Equation 4.

While it may be difficult to distinguish the six different models based on their HR evolutionary tracks or their radial oscillations, their asymptotic gravity mode period spacing shows visible differences. Figure 5 shows the asymptotic period spacing $\Delta\Pi$ (as calculated by Equation 4) as a function of the fundamental RR Lyrae period as the star evolves through the instability strip.

The differences between the models with varying strengths of step overshoot may be difficult to distinguish, but there are clear differences between the models without any additional CBM (Tracks 1-1 and 1-2) and
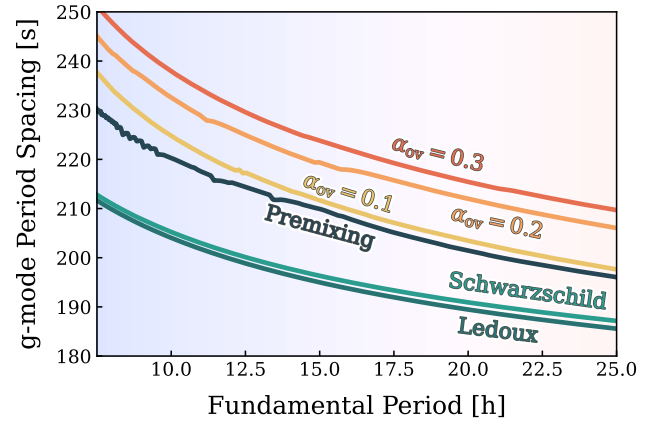
Figure 5. Asymptotic gravity-mode period spacing $\Delta\Pi$ ($\ell = 1$) plotted as a function of the fundamental period. The models with overshoot or premixing show significantly different gravity-mode period spacing than the models without overshoot. The background color shows the spectral type of the star at a given fundamental period.

the other models. Precise measurement of a given star's period spacing and its fundamental period can therefore place constraints on which CBM schemes should best be used to accurately model the star.

6. EFFECT OF MASS AND METALLICITY

As previously noted, RR Lyrae stars typically span a small range of masses ($0.5 \ M_\odot \lesssim M \lesssim 0.8 \ M_\odot$) and metallicities ($0.0001 \lesssim Z \lesssim 0.01$). We evolve six additional models with initial metallicity $Z = 0.002$ and a zero-age core helium-burning mass $M = 0.63 \ M_\odot$ and compare with the models from the previous section; see Table 1 for more details. The evolutionary tracks of these models are shown in Figure 6.

Despite the fact that these models occupy different spaces in the Hertzsprung-Russell diagram, the evolution of the convective core appears to only depend on the CBM scheme. The structure of the convection zone behaves very similarly in these models as compared to the lower mass and metallicity Track 1 models (seen in Figure 2). The models with premixing or overshooting spend a longer time during the core helium fusion phase (~ 50 Myr longer than the no overshoot models). The model with step overshooting spends more time in this phase than the model with premixing (by $\sim 5-15$ Myr). Notably, these models have a larger convective envelope than the Track 1 models. In the case of the no overshoot models, this convective envelope stays throughout the entire core helium fusion phase; for the overshooting and premixing models, this envelope briefly disappears. This could have potential implications for observing gravity modes in such stars. Because gravity modes are damped
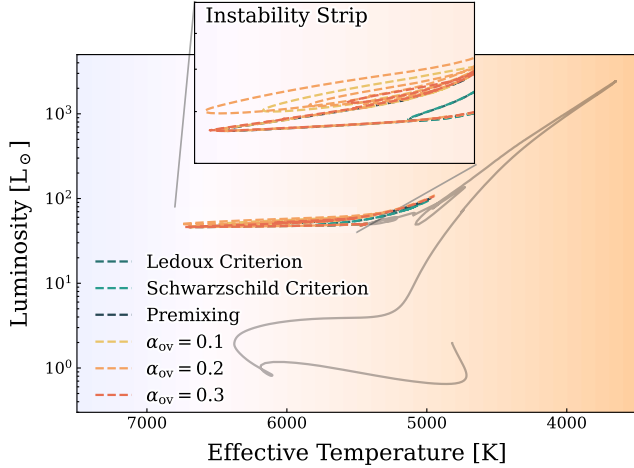
Figure 6. Stellar evolutionary tracks of higher mass and metallicity (M = 0.63 M$_\odot$; Z = 0.002) on the Hertzsprung-Russell diagram with the common track (preceding the helium flash) in black and the six tracks with different CBM schemes during the core helium-burning phase. An inset diagram (5500 K < T < 6800 K; 40 L$_\odot$ < L < 80 L$_\odot$) shows the stellar evolutionary tracks during the classical instability strip. The background is colored by stellar type.

in convection zones, a large outer convective envelope inhibits gravity modes from being observed at the surface. In this case, the mixed mode properties could be more important than the pure gravity mode properties for discerning core physics.

The asymptotic period spacing $\Delta\Pi$ of the star, calculated from Equation 4, is shown as a function of the core helium mass fraction in Figure 7 for three of the Track 1 models and three of the Track 2 models. The figure illustrates how the change in mass and metallicity influences the period spacing. Changes in mass and metallicity produces a nearly negligible effect on the period spacing, while the change in asymptotic period spacing due to different CBM schemes remains clear. Thus, the change in period spacing due to the effects of the different CBM schemes in modeling have a more significant effect than varying mass or metallicity.

Given the presence of a small convective envelope near the surface of the Track 2 models (but the lack thereof in the Track 1 models), this implies that the outer envelope does not significantly affect the asymptotic gravity-mode period spacing. Thus, while there may be many RR Lyrae in which we cannot observe gravity modes, any RR Lyrae in which we may observe gravity modes will likely be representative of the population in terms of the effect of the CBM scheme on the period spacing. This can be further confirmed with a similar analysis presented for a wider grid of models.
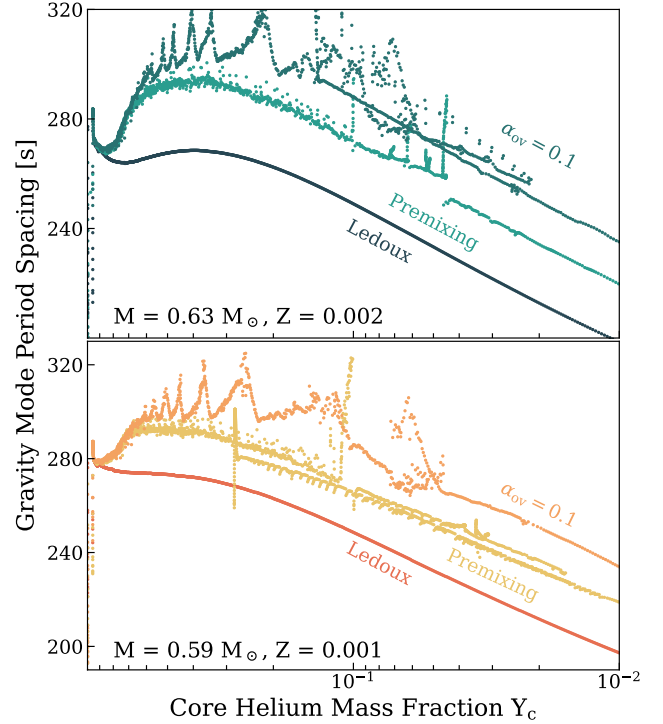
Figure 7. Asymptotic g-mode period spacing $\Delta\Pi$ as a function of the models's core helium mass fraction (a proxy for age during the core helium-burning phase) for the Ledoux, premixing, and step overshoot ($\alpha_{ov} = 0.1$) tracks of two different masses and metallicities (Tracks 1-1, 1-3, 1-4 and 2-1, 2-3, 2-4). In both cases, the different CBM schemes are distinguishable, but the gravity-mode period spacing is not significantly affected by the mass or metallicity change.

7. RR LYRAE IN BINARY SYSTEMS

While RR Lyrae are typically believed to come from old, metal-poor stellar populations, there are observed RR Lyrae with metallicities as high as [Fe/H] = 0.2 (Layden 1995a,b; Liu et al. 2013; Zinn et al. 2019; Bobrick et al. 2024). As metal-rich stars evolve more slowly, stars of RR Lyrae masses typically must be metal-poor to evolve to core helium burning through the classical evolution scenario. Thus, the presence of metal-rich RR Lyrae in the thin disc implies a different formation scenario. The primary star in a binary system transfers mass to the secondary during the primary's red giant phase; the primary, now stripped of its envelope, ignites helium in the core and shrinks, ending the mass transfer and becoming a core helium-burning star (Bobrick et al. 2024). If the amount of envelope stripped is large enough to place the star on the instability strip, but not large enough to fully strip the envelope, the star may become an RR Lyrae. As this can occur at any metallicity of the primary, this formation scenario leads to metal-rich RR Lyrae that formed differently from the

classical formation scenario of RR Lyrae. Several candidates for such binary evolution formed RR Lyrae have been found (Karczmarek et al. 2017; Abdollahi et al. 2025).

One of these RR Lyrae-type pulsators was found to be an "impostor" RR Lyrae (Pietrzyński et al. 2012; Smolec et al. 2013). Its dynamical mass was measured to be $0.26\ M_\odot$, too low to ignite helium. Despite its different internal structure and evolutionary history, as a result of the evolution of the binary system, it exists within the instability strip on the Hertzsprung-Russell Diagram and exhibits RR Lyrae-like pulsations. Some amount of known RR Lyrae (from 0.2% Pietrzyński et al. 2012 to 10% Bobrick et al. 2024) can in fact be these binary-evolution pulsators, possibly contaminating RR Lyrae catalogs used for distance measurements.

Here we construct solar-metallicity stellar models that cross the instability strip after being stripped of their envelopes prior to the helium flash. We initiate these models at a larger mass ($1.2 - 2\ M_\odot$) than can normally produce an RR Lyrae star within the Hubble time. The models undergo a period of constant mass loss prior to the helium flash, bringing them to a typical RR Lyrae mass of $0.55\ M_\odot$. Then, each stripped model is evolved through its core helium-burning phase using (a) no overshoot and (b) step overshoot with $\alpha_{ov} = 0.1$, as in the previous models.

Figure 8 shows the asymptotic g-mode period spacing for the stripped stars during their core helium-burning phase, as well as the asymptotic period spacing for the Track 2 models (which, as discussed in Section 6, is nearly indistinguishable from the original Track 1 models shown in Figure 5). While it is difficult to distinguish between the different initial masses of binary stripped tracks for a given CBM scheme, there is a clear difference between a) the non-stripped tracks and the stripped tracks, and b) the different CBM schemes. Thus, while observations of the period spacing may not be enough to distinguish between different initial masses of the binary system, they can likely distinguish between binary-formed RR Lyrae and isolated RR Lyrae; moreover, for binary-formed RR Lyrae, observations of the period spacing may still be enough to distinguish between different CBM schemes in the core convection zone.

8. EFFECT OF DIFFUSION

To investigate the effects of diffusion, we evolved three models of the original mass ($M = 0.59\ M_\odot$) and metallicity ($Z = 0.001$), including the effects of diffusion in the evolution. The diffusion models with step overshoot and premixing schemes did not have substantially different evolutions of the convective core as compared to the
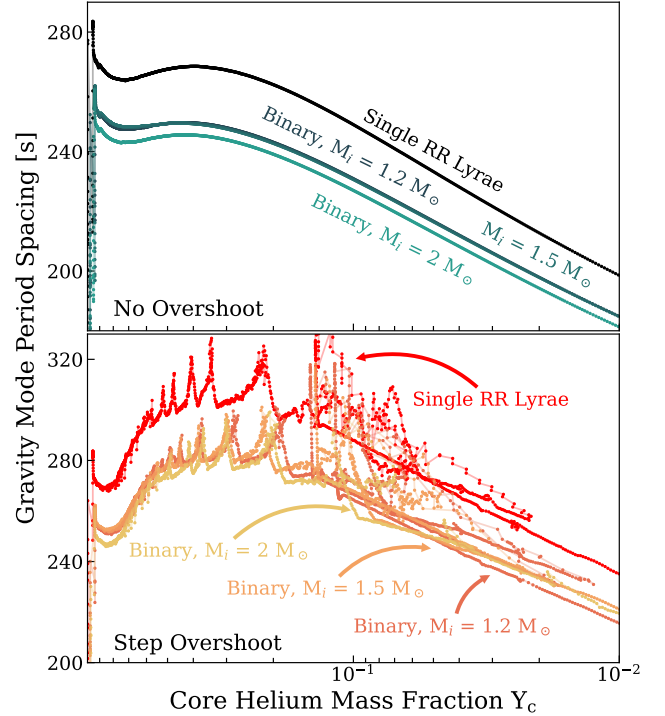

Figure 8. Asymptotic period spacing $\Delta\Pi$ as a function of the models' core helium mass fraction for the stripped models, as well as the single evolution tracks. The gravity-mode period spacing can distinguish between different CBM schemes of a given star as well as between single vs. binary evolution tracks, but it cannot distinguish as easily between different initial masses of the binary evolution stars.

models without diffusion (see Figure 2). The model with no overshoot is significantly different: its convective core grows slowly over the evolution. This difference is noticeable in the asymptotic gravity-mode period spacing, seen in Figure 9. In fact, the model with no overshoot with diffusion is, at later points in the evolution, nearly indistinguishable from the model with step overshoot without diffusion.

9. CONCLUSIONS

We have explored stellar evolution models of RR Lyrae stars with varying methods of convective boundary mixing during the core helium-burning phase: models with no overshoot, models using the convective premixing scheme, and models using step overshoot of varying strengths. These models show vastly different structures in the evolution of the core convective zone, resulting in different helium abundance profiles. These different helium profiles lead to significant differences ($\gtrsim$ 20 s) in gravity modes, which we can observe through the asymptotic period spacing. Moreover, the different models show distinct rates of change of the fundamental period that are large enough (> 0.5 d Myr^{-1}) to
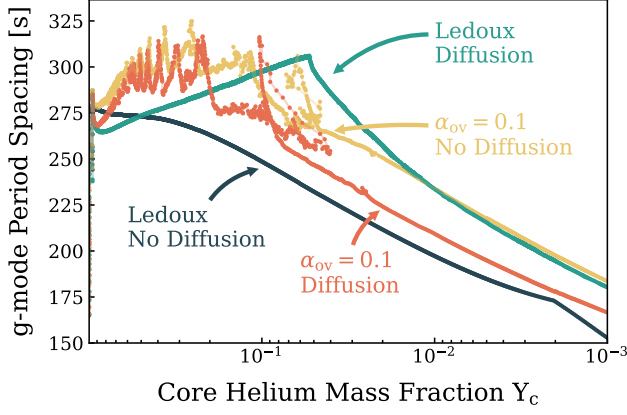
Figure 9. Asymptotic period spacing $\Delta\Pi$ as a function of the models' core helium mass fraction for the Ledoux criterion and step overshoot ($\alpha_{ov} = 0.1$) models with and without diffusion. After the end of the helium breathing pulses (in this case, the RR Lyrae instability strip occurs after $Y_c \lesssim 0.05$), there is almost no distinguishable difference in the period spacing between the model with diffusion without overshoot and the model without diffusion with overshoot.

be detected with long time baselines and constrain the convective treatment of the models through fundamental mode observations alone.

If gravity mode detections are possible for RR Lyrae, then it is possible to use their properties (namely, the period spacing) to constrain the convective boundary mixing scheme used in stellar evolution models. The differences in asymptotic period spacings between, e.g., no overshooting and step overshooting are large enough ($\gtrsim 20$ seconds) to distinguish in observed data. Furthermore, varying the mass and metallicity of the models (within the range of masses and metallicities typical for RR Lyrae stars) does not have a observable impact on the evolution of the convective core or on the period spacings for a given treatment of convection in the model (although it does have impacts on the star's evolutionary track on the Hertzsprung-Russell diagram). While many observed RR Lyrae stars may have gravity modes of amplitudes too low to be observed (due to, for example, outer convection zones), even a small number of RR Lyrae with observed gravity modes can constrain the convective core evolution for this class.

REFERENCES

Abdollahi, H., Molnár, L., & Varga, V. 2025, A&A, 695, L14, doi: 10.1051/0004-6361/202553790

Aerts, C., Christensen-Dalsgaard, J., & Kurtz, D. W. 2010, Asteroseismology, doi: 10.1007/978-1-4020-5803-5

Angulo, C., Arnould, M., Rayet, M., et al. 1999, NuPhA, 656, 3, doi: 10.1016/S0375-9474(99)00030-5

Arellano Ferro, A., Ahumada, J. A., Kains, N., & Luna, A. 2016, MNRAS, 461, 1032, doi: 10.1093/mnras/stw1358

Arellano Ferro, A., Rosenzweig, P., Luna, A., et al. 2018, Astronomische Nachrichten, 339, 158, doi: 10.1002/asna.201813409

Bedding, T. R., Mosser, B., Huber, D., et al. 2011, Nature, 471, 608, doi: 10.1038/nature09935

Bertelli, G., Bressan, A., & Chiosi, C. 1984, in IAU Symposium, Vol. 105, Observational Tests of the Stellar Evolution Theory, ed. A. Maeder & A. Renzini, 333

Blažko, S. 1907, Astronomische Nachrichten, 175, 327, doi: 10.1002/asna.19071752003

Blouin, S., Shaffer, N. R., Saumon, D., & Starrett, C. E. 2020, ApJ, 899, 46, doi: 10.3847/1538-4357/ab9e75

Bobrick, A., Iorio, G., Belokurov, V., et al. 2024, MNRAS, 527, 12196, doi: 10.1093/mnras/stad3996

Borucki, W. J., Koch, D., Basri, G., et al. 2010, Science, 327, 977, doi: 10.1126/science.1185402

Bressan, A., Bertelli, G., & Chiosi, C. 1986, Mem. Soc. Astron. Italiana, 57, 411

Cassisi, S., Potekhin, A. Y., Pietrinferni, A., Catelan, M., & Salaris, M. 2007, ApJ, 661, 1094, doi: 10.1086/516819

Castellani, V., Chieffi, A., Tornambe, A., & Pulone, L. 1985, ApJ, 296, 204, doi: 10.1086/163437

Castellani, V., Giannone, P., & Renzini, A. 1971, Ap&SS, 10, 340, doi: 10.1007/BF00704092

Chadid, M. 2022, ApJ, 925, 114, doi: 10.3847/1538-4357/ac37c0

Charpinet, S., Van Grootel, V., Fontaine, G., et al. 2011, A&A, 530, A3, doi: 10.1051/0004-6361/201016412

Chugunov, A. I., Dewitt, H. E., & Yakovlev, D. G. 2007, PhRvD, 76, 025028, doi: 10.1103/PhysRevD.76.025028

Constantino, T., Campbell, S. W., Christensen-Dalsgaard, J., Lattanzio, J. C., & Stello, D. 2015, MNRAS, 452, 123, doi: 10.1093/mnras/stv1264

Constantino, T., Campbell, S. W., & Lattanzio, J. C. 2017, MNRAS, 472, 4900, doi: 10.1093/mnras/stx2321

Constantino, T., Campbell, S. W., Lattanzio, J. C., & van Duijneveldt, A. 2016, MNRAS, 456, 3866, doi: 10.1093/mnras/stv2939

Córsico, A. H., & Althaus, L. G. 2024, ApJ, 964, 30, doi: 10.3847/1538-4357/ad27d9

Cox, J. P., & Giuli, R. T. 1968, Principles of stellar structure

Cyburt, R. H., Amthor, A. M., Ferguson, R., et al. 2010, ApJS, 189, 240, doi: 10.1088/0067-0049/189/1/240

12

Das, S., Kanbur, S. M., Bellinger, E. P., et al. 2020, MNRAS, 493, 29, doi: 10.1093/mnras/staa182

Deng, L., & Xiong, D. R. 2008, MNRAS, 386, 1979, doi: 10.1111/j.1365-2966.2008.12969.x

Dziembowski, W. A. 2016, Commmunications of the Konkoly Observatory Hungary, 105, 23, doi: 10.48550/arXiv.1512.03708

Eddington, A. S. 1926, The Internal Constitution of the Stars

Fadeyev, Y. A. 2019, Astronomy Letters, 45, 353, doi: 10.1134/S1063773719060021

Ferguson, J. W., Alexander, D. R., Allard, F., et al. 2005, ApJ, 623, 585, doi: 10.1086/428642

Fuller, G. M., Fowler, W. A., & Newman, M. J. 1985, ApJ, 293, 1, doi: 10.1086/163208

Gabriel, M., Noels, A., Montalbán, J., & Miglio, A. 2014, A&A, 569, A63, doi: 10.1051/0004-6361/201423442

Gilligan, C. K., Chaboyer, B., Marengo, M., et al. 2021, MNRAS, 503, 4719, doi: 10.1093/mnras/stab857

Herwig, F., Blöcker, T., & Schönberner, D. 1999, in IAU Symposium, Vol. 191, Asymptotic Giant Branch Stars, ed. T. Le Bertre, A. Lebre, & C. Waelkens, 41, doi: 10.48550/arXiv.astro-ph/9811129

Huber, D., Basu, S., Beck, P., et al. 2019, BAAS, 51, 488, doi: 10.48550/arXiv.1903.08188

Iglesias, C. A., & Rogers, F. J. 1993, ApJ, 412, 752, doi: 10.1086/172958

—. 1996, ApJ, 464, 943, doi: 10.1086/177381

Irwin, A. W. 2004, The FreeEOS Code for Calculating the Equation of State for Stellar Interiors. http://freeeos.sourceforge.net/

Itoh, N., Hayashi, H., Nishikawa, A., & Kohyama, Y. 1996, ApJS, 102, 411, doi: 10.1086/192264

Jermyn, A. S., Schwab, J., Bauer, E., Timmes, F. X., & Potekhin, A. Y. 2021, ApJ, 913, 72, doi: 10.3847/1538-4357/abf48e

Jermyn, A. S., Bauer, E. B., Schwab, J., et al. 2023, ApJS, 265, 15, doi: 10.3847/1538-4365/acae8d

Jurcsik, J., Smitola, P., Hajdu, G., et al. 2015, ApJS, 219, 25, doi: 10.1088/0067-0049/219/2/25

Karczmarek, P., Wiktorowicz, G., Iłkiewicz, K., et al. 2017, MNRAS, 466, 2842, doi: 10.1093/mnras/stw3286

Kippenhahn, R., Weigert, A., & Weiss, A. 2013, Stellar Structure and Evolution, doi: 10.1007/978-3-642-30304-3

Korolik, M. 2025, MESA files, scripts, and data for: On Asteroseismic Probes of Convective Core Boundary Mixing in RR Lyrae Stars, Zenodo, doi: 10.5281/zenodo.15741530

Kuhfuss, R. 1986, A&A, 160, 116

Langanke, K., & Martínez-Pinedo, G. 2000, Nuclear Physics A, 673, 481, doi: 10.1016/S0375-9474(00)00131-7

Layden, A. C. 1995a, AJ, 110, 2288, doi: 10.1086/117690

—. 1995b, AJ, 110, 2312, doi: 10.1086/117691

Ledoux, P. 1947, ApJ, 105, 305, doi: 10.1086/144905

Liu, S., Zhao, G., Chen, Y.-Q., Takeda, Y., & Honda, S. 2013, Research in Astronomy and Astrophysics, 13, 1307, doi: 10.1088/1674-4527/13/11/003

Longmore, A. J., Fernley, J. A., & Jameson, R. F. 1986, MNRAS, 220, 279, doi: 10.1093/mnras/220.2.279

Miglio, A., Montalbán, J., Noels, A., & Eggenberger, P. 2008, MNRAS, 386, 1487, doi: 10.1111/j.1365-2966.2008.13112.x

Montalbán, J., Miglio, A., Noels, A., et al. 2013, ApJ, 766, 118, doi: 10.1088/0004-637X/766/2/118

Mosser, B., Goupil, M. J., Belkacem, K., et al. 2012a, A&A, 540, A143, doi: 10.1051/0004-6361/201118519

—. 2012b, A&A, 540, A143, doi: 10.1051/0004-6361/201118519

Netzel, H., Molnár, L., & Joyce, M. 2023a, MNRAS, 525, 5378, doi: 10.1093/mnras/stad2611

Netzel, H., Molnár, L., Plachy, E., & Benkő, J. M. 2023b, A&A, 677, A177, doi: 10.1051/0004-6361/202245634

Oda, T., Hino, M., Muto, K., Takahara, M., & Sato, K. 1994, Atomic Data and Nuclear Data Tables, 56, 231, doi: 10.1006/adnd.1994.1007

Ostrowski, J., Baran, A. S., Sanjayan, S., & Sahoo, S. K. 2021, MNRAS, 503, 4646, doi: 10.1093/mnras/staa3751

Paxton, B., Bildsten, L., Dotter, A., et al. 2011, ApJS, 192, 3, doi: 10.1088/0067-0049/192/1/3

Paxton, B., Cantiello, M., Arras, P., et al. 2013, ApJS, 208, 4, doi: 10.1088/0067-0049/208/1/4

Paxton, B., Marchant, P., Schwab, J., et al. 2015, ApJS, 220, 15, doi: 10.1088/0067-0049/220/1/15

Paxton, B., Schwab, J., Bauer, E. B., et al. 2018, ApJS, 234, 34, doi: 10.3847/1538-4365/aaa5a8

Paxton, B., Smolec, R., Schwab, J., et al. 2019, ApJS, 243, 10, doi: 10.3847/1538-4365/ab2241

Pedersen, M. G., Aerts, C., Pápics, P. I., & Rogers, T. M. 2018, A&A, 614, A128, doi: 10.1051/0004-6361/201732317

Pietrzyński, G., Thompson, I. B., Gieren, W., et al. 2012, Nature, 484, 75, doi: 10.1038/nature10966

Poutanen, J. 2017, ApJ, 835, 119, doi: 10.3847/1538-4357/835/2/119

Rauer, H., Aerts, C., Cabrera, J., & PLATO Team. 2016, Astronomische Nachrichten, 337, 961, doi: 10.1002/asna.201612408

Rauer, H., Aerts, C., Cabrera, J., et al. 2025, Experimental Astronomy, 59, 26, doi: 10.1007/s10686-025-09985-9

Reed, M. D., Baran, A., Quint, A. C., et al. 2011, MNRAS, 414, 2885, doi: 10.1111/j.1365-2966.2011.18532.x

Ricker, G. R., Winn, J. N., Vanderspek, R., et al. 2015, Journal of Astronomical Telescopes, Instruments, and Systems, 1, 014003, doi: 10.1117/1.JATIS.1.1.014003

Ritter, A. 1880, Annalen der Physik, 246, 130, doi: 10.1002/andp.18802460509

Rogers, F. J., & Nayfonov, A. 2002, ApJ, 576, 1064, doi: 10.1086/341894

Schwarzschild, K. 1906, Nachrichten von der Königlichen Gesellschaft der Wissenschaften zu Göttingen. Math.-phys. Klasse, 195, 41

Smolec, R., Dziembowski, W., Moskalik, P., et al. 2017a, in European Physical Journal Web of Conferences, Vol. 152, European Physical Journal Web of Conferences, 06003, doi: 10.1051/epjconf/201715206003

Smolec, R., Moskalik, P., Kałużny, J., et al. 2017b, MNRAS, 467, 2349, doi: 10.1093/mnras/stx088

Smolec, R., Pietrzyński, G., Graczyk, D., et al. 2013, MNRAS, 428, 3034, doi: 10.1093/mnras/sts258

Stock, J., & Wroblewski, H. 1972, Publications of the Department of Astronomy University of Chile, 2, 59

Sweigart, A. V., & Demarque, P. 1973, in Astrophysics and Space Science Library, Vol. 36, IAU Colloq. 21: Variable Stars in Globular Clusters and in Related Systems, ed. J. D. Fernie, 221, doi: 10.1007/978-94-010-2590-4_32

Tassoul, M. 1980, ApJS, 43, 469, doi: 10.1086/190678

Townsend, R. H. D., Goldstein, J., & Zweibel, E. G. 2018, MNRAS, 475, 879, doi: 10.1093/mnras/stx3142

Townsend, R. H. D., & Teitler, S. A. 2013, MNRAS, 435, 3406, doi: 10.1093/mnras/stt1533

Zinn, R., Chen, X., Layden, A. C., & Casetti-Dinescu, D. I. 2019, Monthly Notices of the Royal Astronomical Society, 492, 2161, doi: 10.1093/mnras/stz3580